

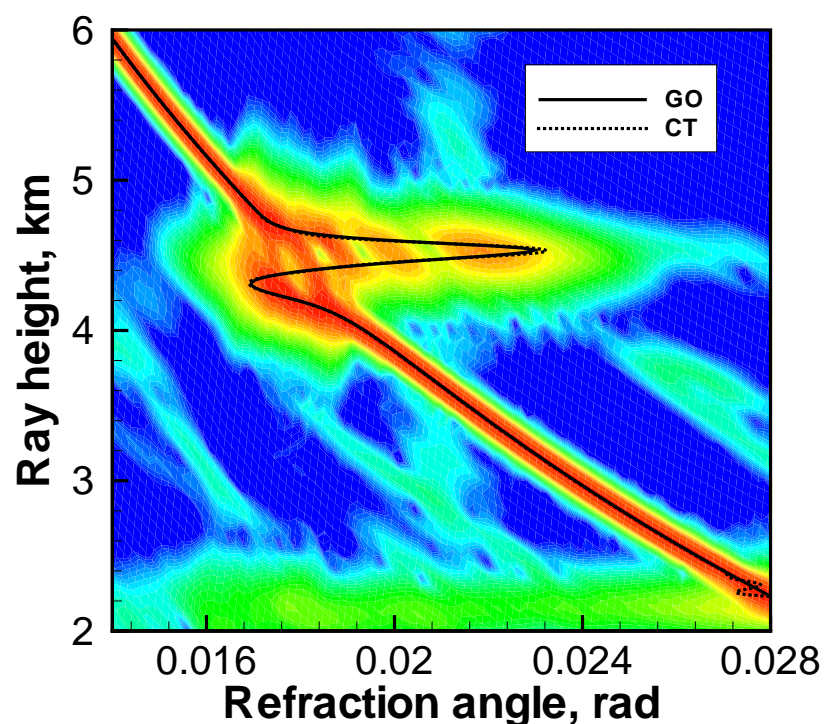
Scientific Report 05-06

Radio Holographic Filtering of Noisy Radio Occultations

M. E. Gorbunov¹ and K. B. Lauritsen²

¹*Institute for Atmospheric Physics, Moscow 119017, Russia, gorbunov@dkrz.de*

²*Danish Meteorological Institute, DK-2100 Copenhagen, Denmark, kb1@dmi.dk*





Colophone

Serial title:

Scientific Report 05-06

Title:

Radio Holographic Filtering of Noisy Radio Occultations

Subtitle:

Authors:

M. E. Gorbunov¹ and K. B. Lauritsen²

¹*Institute for Atmospheric Physics, Moscow 119017, Russia, gorbunov@dkrz.de*

²*Danish Meteorological Institute, DK-2100 Copenhagen, Denmark, kbl@dmi.dk*

Other Contributors:

Responsible Institution:

Danish Meteorological Institute

Language:

English

Keywords:

Url:

www.dmi.dk/dmi/dmi-publikationer.htm

ISSN:

1399-1949

ISBN:

87-7478-525-7

Version:

Website:

www.dmi.dk

Copyright:

Danish Meteorological Institute



Contents

Colophone	2
1 Introduction	4
2 Inversion of data without noise	5
3 Phase models	6
4 Radio holographic noise filtering	7
5 Inversion of noisy data	7
6 Conclusions	9
References	10

Radio Holographic Filtering of Noisy Radio Occultations

M. E. Gorbunov¹ and K. B. Lauritsen²

¹*Institute for Atmospheric Physics, Moscow 119017, Russia, gorbunov@dkrz.de*

²*Danish Meteorological Institute, DK-2100 Copenhagen, Denmark, kbl@dmi.dk*

Abstract

We investigate algorithms for filtering noisy radio occultation data with atmospheric multipath behavior in order to improve the accuracy of the inversion based on canonical transform/full spectrum methods. The noise filtering procedure uses the compression of the signal spectrum by multiplying it with a reference signal, Fourier filtering of the narrow-banded signal, and decompression of its spectrum. We study filtering in the time domain and in the impact parameter domain. Our results show that the inversion methods are able to handle additive white noise and high resolution bending angle profiles are obtained. For comparison we also present results where the inversion of multipath behavior is based on using phase data only.

1 Introduction

Recently radio occultation data with atmospheric multipath behavior have attracted much attention. It has been shown that canonical transform/full spectrum inversion (CT, FSI, CT2) methods based on Fourier integral operators can effectively unfold multipath behavior [1, 2, 3]. Furthermore, this approach gives a high accuracy for the retrieved bending angle profiles. Some investigations of the CT/FSI inversion in the presence of white noise were performed in [4].

In the present work, we investigate the effect of noise on the inversion of radio occultations by CT/FSI canonical transform methods. We introduce radio-holographic filtering methods that use reference signals for compression of the spectrum of radio occultation measurements and investigate how this affects the resolution. We find that it is possible to obtain high resolution unfolding of multipath behavior even in the presence of relatively strong noise. For comparison, we also study the case where the inversion is based on the phase data without using the amplitude. It is still possible to unfold the multipath behavior without using amplitude data but it results in reduced accuracy for the bending angle profiles. By applying a model for the amplitude (or using a strongly smoothed version of the measured, noisy amplitude) one can obtain an approximately constant CT/FSI amplitude. Our investigations are based on simulated radio occultation data with multipath behavior.

For a spherical symmetric atmosphere the impact parameter, p , uniquely defines a ray [1] (with horizontal gradients the assumption will be fulfilled to a good approximation). Thus, the procedure for unfolding atmospheric multipath behavior in radio occultations consists in mapping the measured field $u(t) = A(t) \exp(i\phi(t))$ to the p -representation, $w(p)$, using methods based on Fourier integral operators (FIO) and canonical transforms (FSI [2], CT2 [3, 5]). The resulting operator can be written

as the composition of multiplication with a reference signal $\exp(ik \int f(Y) dY)$, the Fourier transform, and an amplitude factor:

$$\Phi_2 u(\tilde{p}) = \sqrt{\frac{-ik}{2\pi}} a_2(\tilde{p}, Y_s(\tilde{p})) \int \exp(-ik\tilde{p}Y) \exp\left(ik \int_0^Y f(Y') dY'\right) u(Y) dY. \quad (1.1)$$

The coordinate Y depends on time, $Y = Y(t)$, and the stationary phase point $Y_s(\tilde{p})$ equals $-\tilde{\xi}$, where the momentum $\tilde{\xi}$ is the derivative of the eikonal of the integral term in (1.1):

$w(\tilde{p}) \equiv \Phi_2 u(\tilde{p}) = B(\tilde{p}) \exp(ik\Psi(\tilde{p}))$, $\tilde{\xi} \equiv d\Psi(\tilde{p})/d\tilde{p}$. This operator maps the wave field to the representation of the approximate impact parameter \tilde{p} . Knowing \tilde{p} , the exact p can be obtained (practically, the difference between them is small and can be neglected). The factor $a_2(\tilde{p}, Y_s(\tilde{p}))$ is the amplitude function of the FIO operator and is needed in order to ensure energy conservation (see e.g. [3, 5]). The bending (or refraction) angle, $\epsilon(p)$, is obtained from the derivative of the phase of $w(p)$ in combination with the geometric formula relating the various angles in the occultation geometry.

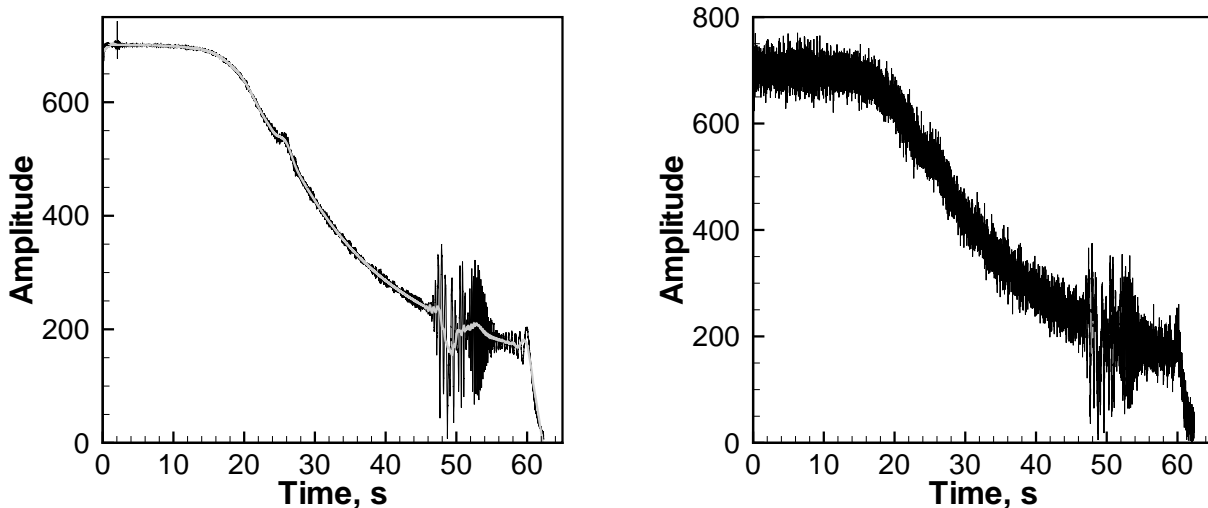


Figure 1.1: Amplitude of simulated field without noise with multipath behavior (left). The superimposed line (light gray) is a strongly smoothed version of the amplitude. The simulated field with additive Gaussian white noise with a strength of 30 [4] (right).

2 Inversion of data without noise

In Fig. (1.1) we show the amplitude of a simulated field with a simple atmospheric multipath behavior that we used in our investigations. The simulation have been performed by a combined multiple phase screen method and asymptotic modeling [3].

In Figs. (2.1)-(2.3) we show the retrieved bending angle profiles $\epsilon(p)$ with CT and GO (geometric optics) algorithms (without doing noise filtering). The left panels also show the (sliding) spectra in the (p, ϵ) -space (where ray height is p minus the Earth local curvature radius). The right panels show the CT amplitudes as function of ray height. One observes that high resolution bending angle profiles can be obtained even in the case where the amplitude is not used. With the strongly smoothed amplitude, it is observed that the CT amplitude is not constant in the multipath region (in the p -representation). This reflects the fact that the strong smoothed version of the simulated amplitude does not respect the conservation of energy.

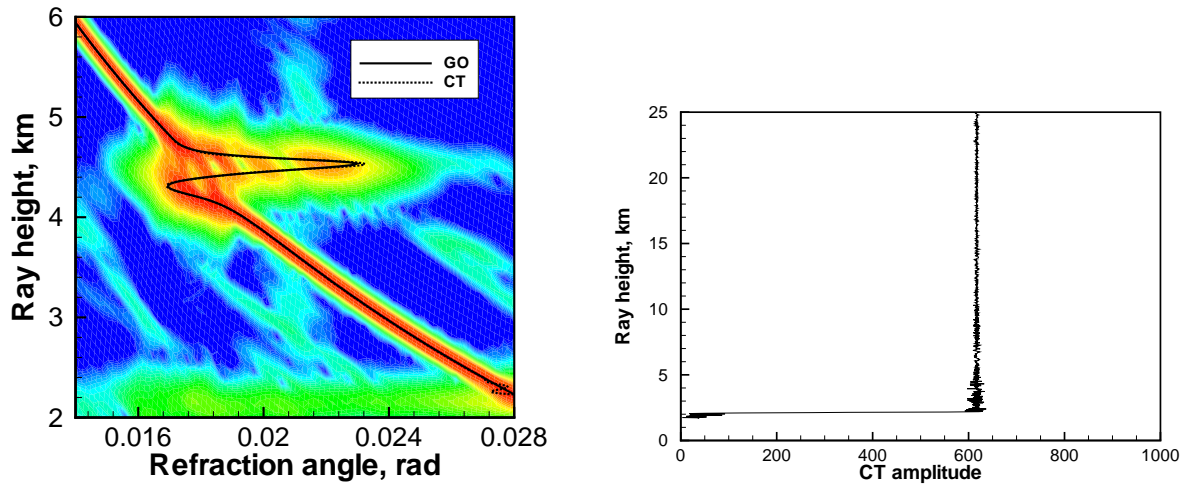


Figure 2.1: Bending angle and (p, ϵ) -spectrum (left) and CT amplitude as function of ray height (right). The results are obtained directly from the simulated amplitude.

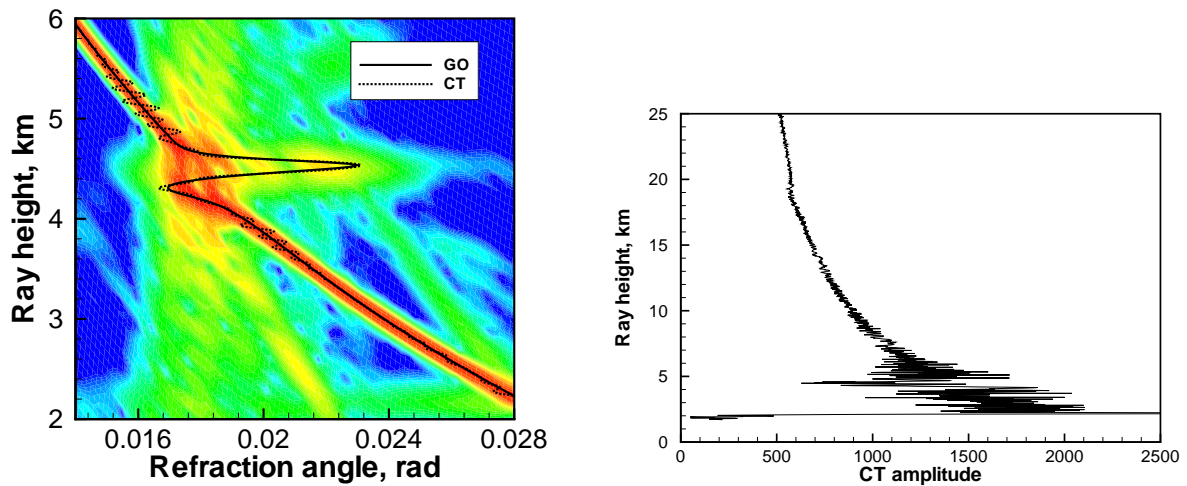


Figure 2.2: Bending angle and (p, ϵ) -spectrum (left) and CT amplitude as function of ray height (right). The results are obtained by using a constant amplitude ($A \equiv 1$).

3 Phase models

We construct smooth models for the phase variations, $\phi_m(t)$ and $\Psi_m(p)$, based on the measured signal and on the retrieved bending angle profile without doing any noise filtering. The measured signal $u(t)$ and the transformed signal $w(p)$ are then multiplied by the phase model reference signals as follows:

$$u(t) \rightarrow u_m(t) \equiv u(t) \exp(-i\phi_m(t)), \quad (3.1)$$

where the phase model $\phi_m(t)$ is obtained by smoothing the phase of the measured wave field $u(t)$. Analogously, for the $w(p)$ field:

$$w(p) \rightarrow w_m(p) \equiv w(p) \exp(-ik\Psi_m(p)), \quad (3.2)$$

where the phase model $\Psi_m(p)$ is obtained by smoothing the phase of $w(p)$.

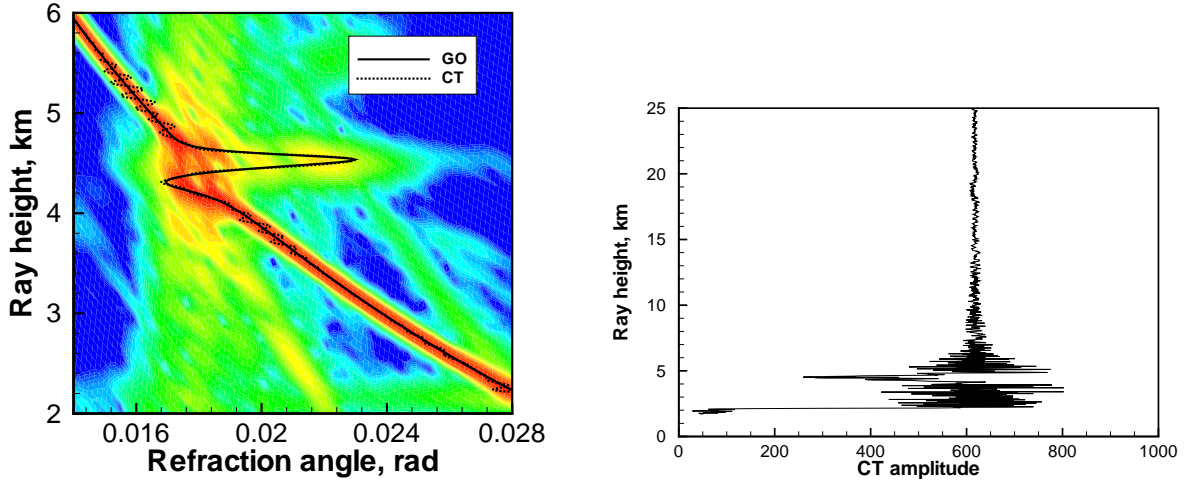


Figure 2.3: Bending angle and (p, ϵ) -spectrum (left) and CT amplitude as function of ray height (right). The results are obtained by using a strongly smoothed version of the simulated amplitude.

4 Radio holographic noise filtering

The filtering of the noisy signals are done in three steps: first, the signals are multiplied by reference signals. This step ensures that the spectrum will be narrow-banded. Next, the modified signals are Fourier transformed, a Gaussian weighting function applied, and inverse Fourier transformed. Finally, the reference signals are removed. In schematized form, the steps are as follows for the noise filtering in the t -domain:

$$u(t) \rightarrow u_m(t) \quad [\text{add } \phi_m(t)] \quad (4.1)$$

$$\rightarrow \tilde{u}_m(\omega) \quad [F] \quad (4.2)$$

$$\rightarrow \tilde{u}_m^{F_t}(\omega) \equiv \tilde{u}_m(\omega) \exp(-\omega^2/2\sigma_\omega^2) \quad [\text{Gaussian filtering}] \quad (4.3)$$

$$\rightarrow u_m^{F_t}(\omega) \quad [F^{-1}] \quad (4.4)$$

$$\rightarrow u^{F_t}(t) \quad [\text{remove } \phi_m(t)] \quad (4.5)$$

Next, apply Φ_2 in order to obtain the field in the p -representation, $w^{F_t}(p)$, and finally, obtain the bending angle $\epsilon^{F_t}(p)$ from the derivative of the phase of $w^{F_t}(p)$.

For the noise filtering in the p -domain it reads:

$$w(p) \rightarrow w_m(p) \quad [\text{add } \Psi_m(p)] \quad (4.6)$$

$$\rightarrow \tilde{w}_m(\xi) \quad [F] \quad (4.7)$$

$$\rightarrow \tilde{w}_m^{F_p}(\xi) \equiv \tilde{w}_m(\xi) \exp(-\xi^2/2\sigma_\xi^2) \quad [\text{Gaussian filtering}] \quad (4.8)$$

$$\rightarrow w_m^{F_p}(\xi) \quad [F^{-1}] \quad (4.9)$$

$$\rightarrow w^{F_p}(p) \quad [\text{remove } \Psi_m(p)] \quad (4.10)$$

Next, obtain the bending angle $\epsilon^{F_p}(p)$ from the derivative of the phase of $w^{F_p}(p)$.

5 Inversion of noisy data

The results of our noise filtering procedure are shown in Figs. (5.1)-(5.3) where we show the retrieved bending angle profiles, the (p, ϵ) -spectrum for the noisy simulation, and the CT/FSI

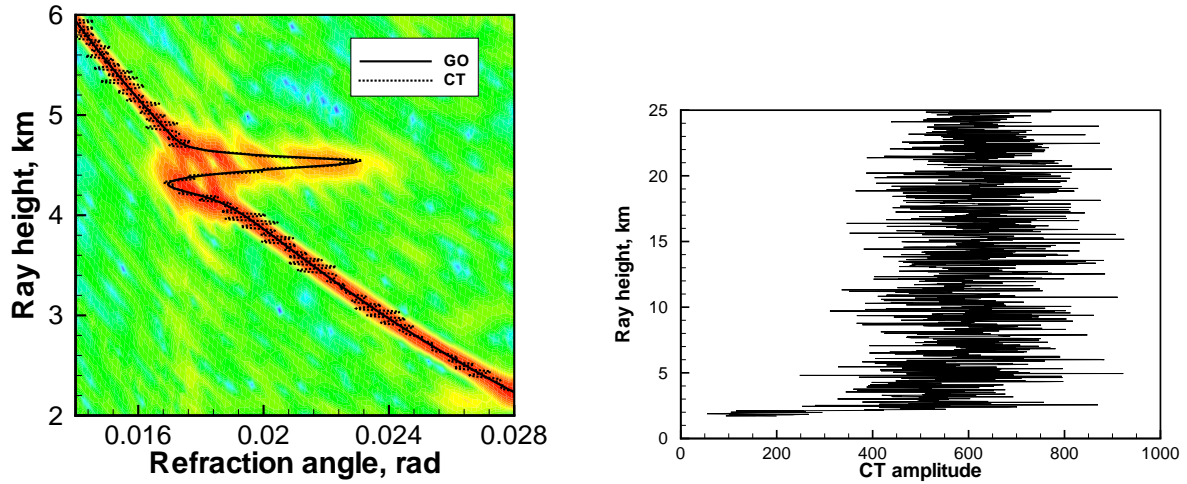


Figure 5.1: Bending angle and (p, ϵ) -spectrum (left) and CT amplitude as function of ray height (right). The bending angle $\epsilon(p)$ and CT amplitude are obtained without any noise filtering.

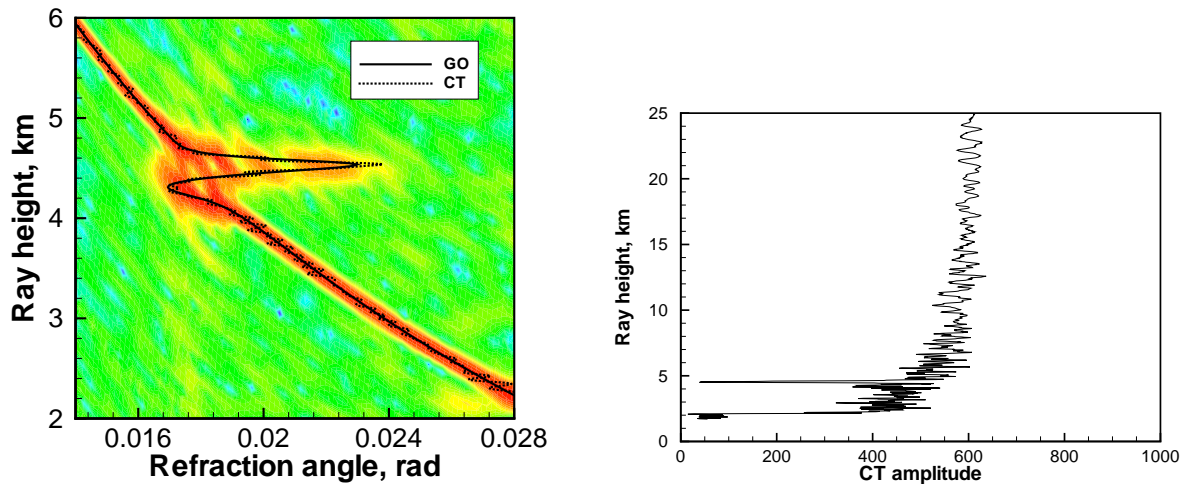


Figure 5.2: Bending angle and (p, ϵ) -spectrum (left) and CT amplitude as function of ray height (right). The bending angle $\epsilon^{F_t}(p)$ and CT amplitude are obtained with the $\phi_m(t)$ phase model.

amplitudes. The results have been obtained by using a smoothing window of a size corresponding to about 30 m. The phase model $\phi_m(t)$ has been obtained by smoothing at the scale 2 sec (corresponding to about 4 km in the vertical scale in the sliding spectra). The width of the filter was chosen to be $\sigma_\omega = 200 \text{ s}^{-1}$, corresponding to impact parameter intervals of $\Delta p \approx 4 \text{ km}$ ($\omega \approx kp\Omega$, with $k \approx 33 \text{ m}^{-1}$, and the derivative of the satellite-to-satellite angle θ being approximately $\Omega = d\theta/dt \approx 0.0015 \text{ rad/s}$ for the simulation we have investigated). For $\Psi_m(p)$, the smoothing scale was chosen to correspond to the radio-holographic filter width, thus $\sigma_\xi = 0.005 \text{ rad}$.

Fig. (5.2) shows that the noise filtering has removed some energy from the signal since the CT amplitude is no longer (approximately) constant. The sharp decrease in amplitude seen around 5 km signals that the original multipath behavior (in the t -space) has been slightly corrupted by the Gaussian filtering (in the ω -space). This can be traced to the fact that the width of the multipath spectrum has been larger than the used noise filtering width σ_ω . Phrased differently, the unfolding of the multipath behavior is not complete in the ω -space, therefore the spectrum will be slightly broader

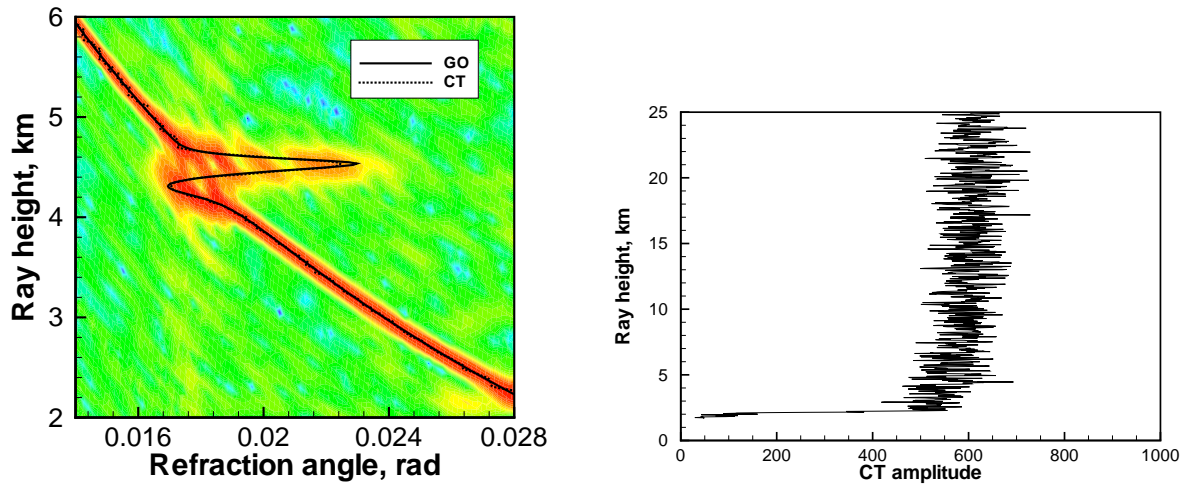


Figure 5.3: Bending angle and (p, ϵ) -spectrum (left) and CT amplitude as function of ray height (right). The bending angle $\epsilon^{F_p}(p)$ and CT amplitude are obtained with the $\Psi_m(p)$ phase model.

in the multipath region than outside it (i.e., in the single path regions) and accordingly the weighting with a Gaussian can slightly cut off the spectrum width.

On the contrary, the filtering in the ξ -space, using the impact parameter reference model $\Psi_m(p)$, has not corrupted the multipath spectrum (Fig. (5.3)). This is also to be expected, since the multipath behavior will be completely unfolded in the p -representation. Thus, the field $\tilde{w}(\xi)$ will be more narrow-banded than $\tilde{u}(\omega)$ and therefore the noise filtering of $\tilde{w}(\xi)$ will not interfere with the multipath behavior. In this sense, the filtering in the ξ -space is optimal.

We have carried out simulations for different strengths of the noise level. We find that the $\phi_m(t)$ filtering breaks down for strengths about 100 whereas the $\Psi_m(p)$ filtering breaks down for strengths about 50. Thus, the filtering in the ω -domain seems to be more robust (but note the fact that the spectrum in this space is broader and thus the filtering may slightly disturb the multipath structure). One way to interpret this is that the (small) suppression of some of the multipath structures seems to have created a slightly more robust signal.

6 Conclusions

We have investigated the effect of noise on CT/FSI retrieval methods. To this end, we have introduced a filtering approach based on phase models. The noise reduction is performed in either the ω -space (conjugate to the time domain) or the ξ -space (conjugate to the impact parameter domain). We find that high resolution bending angle profiles can be obtained, even in the presence of relatively strong noise levels. Thus, FIO-based retrieval methods are robust with respect to additive wide band noise. However, the noise filtering breaks down for very high noise levels.

We also investigated the case where the inversion is performed using the phase signal alone (and a constant or strongly smoothed amplitude signal). In such cases, the CT/FSI amplitude is no longer constant, signalling that the inversion did not respect the conservation of energy. On the other hand, by imposing a constant CT/FSI amplitude, and mapping such a signal back to the time domain, one can construct a model for the measured amplitude that can reveal the structure of the multipath behavior in the signal.

References

- [1] M. E. Gorbunov (2002) Radio-holographic analysis of Microlab-1 radio occultation data in the lower troposphere. *J. of Geophys. Res.* 107(D12), 10.1029/2001JD000889; M. E. Gorbunov (2002) Canonical transform method for processing GPS radio occultation data in the lower troposphere. *Radio Science* 37(5), 1076, 10.1029/2000RS002592
- [2] A. S. Jensen, M. S. Lohmann, H.-H. Benzon, and A. S. Nielsen (2003) Full spectrum inversion of radio occultation signals. *Radio Science* 38(3), 1040, 10.1029/2002RS002763
- [3] M. E. Gorbunov and K. B. Lauritsen (2004) Analysis of wave fields by Fourier integral operators and their application for radio occultations. *Radio Science* 39(4), RS4010, 10.1029/2003RS002971
- [4] M. E. Gorbunov, H.-H. Benzon, A. S. Jensen, M. S. Lohmann, and A. S. Nielsen (2004) Comparative Analysis of Radio Occultation Processing Approaches Based on Fourier Integral Operators. *Radio Science* 39(6), RS6004, 10.1029/2003RS002916
- [5] M. E. Gorbunov and K. B. Lauritsen (2005) Canonical Transform Methods for Analysis of Radio Occultations, in “Earth Observation with CHAMP: Results from Three Years in Orbit”, eds. C. Reigber, H. Luehr, P. Schwintzer, and J. Wickert, pp.519-524, Springer Verlag, Berlin

Acknowledgements

This work has been supported by the EUMETSAT GRAS Meteorology SAF project.

Previous reports

Previous reports from the Danish Meteorological Institute can be found on:
<http://www.dmi.dk/dmi/dmi-publikationer.htm>